Journal of Sound and Vibration (1998) **211**(3), 481–494

ON ANALOG FEEDBACK CONTROL FOR MAGNETOSTRICTIVE TRANSDUCER LINEARIZATION

D. L. Hall and A. B. Flatau

Department of Aerospace Engineering and Engineering Mechanics, *Iowa State University*, 2019 *Black Engineering Building*, *Ames*, *Iowa* 50011, *U.S.A.*

(*Received* 10 *July* 1996, *and in final form* 4 *March* 1997)

The magnetostrictive transducer output force, displacement, and bandwidth characteristics are well suited for a variety of active vibration control applications. However, their use is limited in part because these transducers are known to be non-linear. The transducer in this study is assumed to be a linear system and its output harmonics are assumed to be disturbance inputs. Two feedback control models are proposed and one is used to obtain expressions for predicting the change in harmonic amplitudes of displacement and acceleration as functions of frequency and parameters for the controller, load, and transducer. An approach based on magnetostrictive transduction modelling is presented for experimentally determining appropriate transducer model parameters for use in the feedback control model. Experimental measurements using simple, analog, PD (proportional plus derivative) acceleration feedback control are presented to validate the expressions. The closed loop feedback control system model resulted in predicted changes in harmonic acceleration amplitudes ranging from $+2$ to -30 dB (depending upon the frequency of the disturbance input) that were verified experimentally. A significant extension of the linear range of transducer behavior, due to feedback control, is also demonstrated.

1. INTRODUCTION

Magnetostrictive materials are the magnetic analogs of the more familiar piezoelectric materials. Magnetostrictives transduce strain and magnetic energies. Terfenol-D† is a "giant" magnetostrictive material offering mechanical strains of up to 2000×10^{-6} m/m (2000 μ strain). Magnetostrictive transducers constructed using Terfenol-D rods of lengths up to 24 cm offer displacements based on approximately ± 500 μ strain with output over a bandwidth from DC to over 20 kHz. In spite of non-linearities inherent in the cyclic strain of this magnetic material, it has received considerable attention for use in sonar applications, and is beginning to be recognized as an attractive material for design of certain smart structural system.

A non-linarity of particular importance when using Terfenol-D transducers is wave form distortion. The distortion is a result of a quadratic non-linear strain versus magnetization relationship and magnetic hysteresis occurring within the Terfenol-D. The net result is varying amplitude integer harmonics present in the transducer voltage, current, and output velocity. These amplitudes typically increase with increasing excitation level.

† Terfenol-D is a magnetostrictive material which was discovered at the Naval Ordinance Laboratory and it is produced by alloying the rare-earths terbium and dysprosium with iron. Thus, Terfenol-D stands for Ter(bium) + Fe(iron) + nol (Naval Ordinance Laboratory) + D(ysprosium). It has been commercially available since the late 1980s. An authoritative discussion of the physics of the material is available in reference [3].

0022–460X/98/130481 + 14 $25.00/0/sv971322

Magnetostrictive transducers are traditionally considered as being reasonable approximations of linear systems at low drive amplitudes [1–3] and as becoming very non-linear at high drive amplitudes [3–5]. (Linear in the sense that sinusoidal input produces sinusoidal output.) These are all relative terms. A more concrete example is shown in Figures 1(a) and 1(b) which respectively display plots of percent displacement from current ($\|u/I\|$ as a percentage of the displacement measured when driven at 800 mA) and percent harmonic distortion (%HD) versus drive current amplitude. The data in Figure 1 were calculated from information given in reference [2, Table 5.1], which also provides a full description of the transducer used. For these tests, the transducer was driven by 200 Hz sinusoidal drive currents of various amplitudes using an amplifier with a current control module. As operated, a "high" drive current amplitude for this transducer was 800 mA zero to peak. Measured acceleration autospectral density functions (0–2 kHz) were obtained for each drive-current amplitude. Displacement from current values were those corresponding to the 200 Hz component only, and all are shown as percentages of the 800 mA value (11·2 μm/A) and thus show the change in output sensitivity as a function of input. %HD was calculated as the ratio of the summation of the harmonic amplitudes to that of all of the amplitudes (the harmonics occurred at integer multiples of the fundamental).

Displacement per amp is clearly not a constant for this transducer. Driving this system harder produces significant gains in output displacement per unit input current. (Linearization of this output/input relationship is not addressed in this study.) Unfortunately, wave form harmonic distortion also increases with increasing drive current amplitudes. Thus, although significant increases in output displacement and force (and therefore control authority) occur with increasing drive amplitudes (Fig. 1(a)), increased harmonic distortion with increasing drive amplitudes (Figure 1(b)) limits the utility of these transducers in vibration control applications, where undesirable excitation of structural modes by transducer harmonics can occur. Thus, one would like to decrease the output harmonics in order to take advantage of the significant increases in the useful displacement range of transducer operation with higher drive amplitudes. That was the impetus for the investigation reported here.

2. MODELLING APPROACH

The magnetostrictive transducer is modelled as a linear system satisfying a pair of linear simultaneous equations. The harmonic frequencies present in the state variables will be thought of as disturbances.

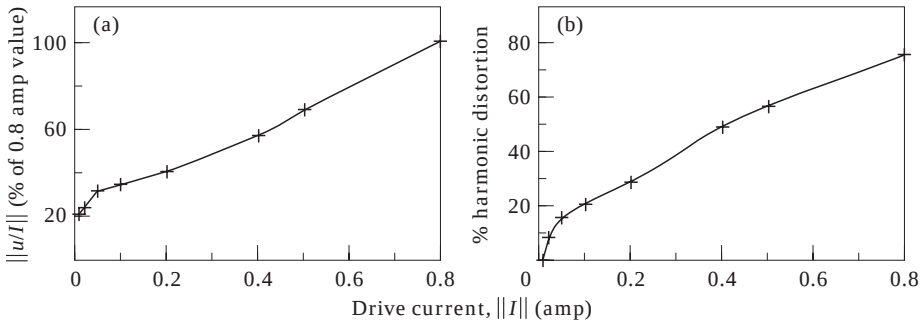

Figure 1. (a) Displacement from drive current and (b) harmonic distortion at different 200 Hz drive current amplitudes as a percentage of their respective 0·8 Amp values.

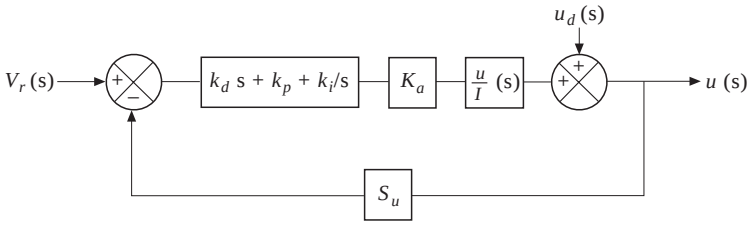

Figure 2. Block diagram of feedback system assuming a PID controller, a current controlled amplifier of gain K_a, a displacement sensor of sensitivity S_u, and disturbance displacements, u_d.

The canonical form of the transduction equations, as applied to a magnetostrictive transducer, is [1]

$$V = Z_e I + T_{em} v, \qquad 0 = T_{me} I + z_x v, \tag{1a, b}$$

where V = voltage across the transducer leads (volts); Z_e = blocked electrical impedance of the transducer (blocked physically, i.e., the electrical impedance one would measure if the output velocity were held at zero) = $sL_e + R_e$, where s is the Laplace operator, L_e is the blocked electrical inductance (henries) and R_e is the dc resistance of the wound wire solenoid, in units of ohms (Ω); I = electric current passing through the wound wire solenoid, amperes (A); T_{em} = the transduction coefficient, electrical due to mechanical, in units of volts per meter per second (V/(m/s)); v = the mechanical output velocity of the transducer (m/s); T_{me} = the transduction coefficient, mechanical due to electrical (N/A); and z_x = the mechanical impedance, based on velocity, of the transducer and the load, which, in its simplest applicable form is given as: $z_x = sm_x + b_x + k_x$ /s, where m_x is the sum of the internal dynamic mass of the transducer plus the load mass (kg); b_x is the sum of the damping within the transducer and that due to the load (N/(m/s)), and k_x is the combined stiffness of the transducer and the load, (N/m). It is shown in the literature [1, 2, 6] that for magnetostrictive transducers, ignoring eddy current effects, $T_{em} = -T_{me}$ = a drive amplitude dependent pseudoconstant. Thus, for transduction, T defined as $T = T_{em} = -T_{me}$ is used. Using this substitution in equations (1), one can solve for the useful fundamental transducer relationships when operating in its linear range given in equations (2–6):

$$\frac{v}{I}(s) = \frac{T}{z_x}, \qquad \frac{V}{I}(s) = \frac{z_e z_x + T^2}{z_x}, \qquad \frac{v}{V}(s) = \frac{(v/I)}{(V/I)} = \frac{T}{Z_e z_x + T^2}, \tag{2–4}$$

$$\frac{u}{V}(s) = \frac{1}{s}\frac{v}{V} = \frac{T}{s(Z_e z_x + T^2)}, \qquad \frac{a}{V}(s) = \frac{sv}{V} = \frac{sT}{Z_e z_x + T^2}, \tag{5, 6}$$

where u is transducer output displacement (m); a is transducer output acceleration (m/s^2); equations presented are functions of the Laplacian operator s. All of these equations will be useful when modelling the transducer as part of the overall controlled system.

2.1. FEEDBACK MODELS USING A CURRENT-CONTROL AMPLIFIER

The magnetic field applied inside a transducer is directly proportional to the product of the number of turns per meter of the transducer's solenoid and the current through the solenoid. Figure 2 shows a block diagram for the system consisting of a PID (proportional, integral, and derivative) controller; a current-controlled amplifier, of gain K_a (A/V); the transducer (expressed as displacement per ampere = equation (2) divided by s); disturbance displacements, u_d ; and a displacement transducer of sensitivity, s_u (V/m). The reference signal is shown as V_r ; it is the input for the controlled system. Using the

definitions for the impedances (Z_e and z_x) detailed in equations (1), the system transfer function u/V_r is calculated as

$$\frac{u}{V_r}(\mathrm{s}) = [(\mathrm{s}k_d + k_p + k_i/\mathrm{s})K_a\,(T/\mathrm{s}z_x)]/[1 + (\mathrm{s}k_d + k_p + k_i/\mathrm{s})K_a\,(T/\mathrm{s}z_x)S_u]$$

which reduces to

$$\frac{u}{V_r}(\mathrm{s}) = \frac{(\mathrm{s}^2k_d + \mathrm{s}k_p + k_i)K_a\,T}{\mathrm{s}^3m_x + \mathrm{s}^2(b_x + k_d\,K_a\,TS_u) + \mathrm{s}(k_x + k_p\,K_a\,TS_u) + k_i\,K_a\,TS_u}. \tag{7}$$

This function has two, possibly complex zeros in the LHP (left half-plane) given as

$$\mathrm{s}_{1,2} = [-k_p \pm (k_p^2 - 4k_d\,k_i)^{1/2}]/2k_d$$

and the Routh–Hurwitz criteria [1] guarantees that it will have its three poles in the LHP (be stable) if

$$k_x\,b_x + k_d\,(k_x + k_p\,K_a\,TS_u)K_a\,TS_u + k_p\,k_x\,K_a\,TS_u > m_x\,k_i\,K_a\,TS_u.$$

This derivation assumes that the system parameters are constants, independent of drive magnitude and frequency. These are tenuous assumptions when dealing with Terfenol-D transducers, as discussed in references [8, 9]. (T, R_e, L_e, K_a, and k_x are all of particular concern with these actuators.)

Other relations could be developed assuming one had a current-controlled amplifier that was robust enough to be a reasonable approximation of the constant K_a. That was not the case in this investigation. Although current control was attempted, magnetostrictive transducers are very active loads and the amplifier current output did not follow the input signal sufficiently at different frequencies to study the case of constant K_a.

2.2. FEEDBACK MODELS USING A VOLTAGE-CONTROLLED AMPLIFIER

The rest of the work presented employs models based on a voltage-controlled amplifier. This model is more complex in that the applied magnetic field in the transducer is now proportional to the product of the turns per meter of the solenoid, the voltage across the solenoid, and the inverse of equation (3), a complex valued electrical impedance function that varies with operating conditions.

In addition, emphasis will be placed on oscillatory drive conditions using an accelerometer as the feedback transducer. This was done for two reasons: (1) the equipment was available, (2) small amplitude disturbance displacements are anticipated and using an accelerometer as the feedback transducer exploits the ω^2 signal amplification inherent to acceleration measurements.

Figure 3 is a block diagram of the feedback system assuming a voltage-controlled amplifier. (Voltage was much easier for controlling the amplifier used than current when

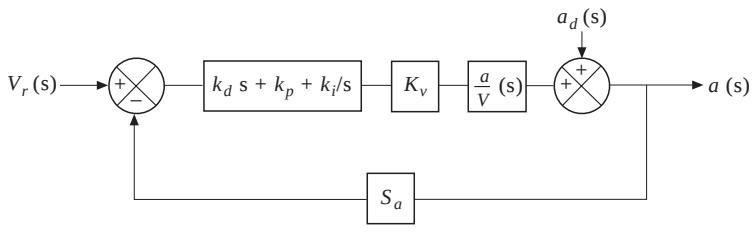

Figure 3. Block diagram of feedback system assuming a PID controller, a voltage-controlled amplifier of gain K_V, an acceleration sensor of sensitivity S_a, and disturbance accelerations, a_d.

driving a Terfenol-D transducer.) The transducer's transfer function for acceleration per volt is given in equation (6). Using the PID controller defined in Figure 3, the relations for the impedances detailed below equations (1) and (6), the transfer function for the closed loop system, as a/V_r, is given as

$$\frac{a}{V_r}(\mathrm{s}) = \frac{(k_d\,\mathrm{s} + k_p + k_i/\mathrm{s})K_V\,(\mathrm{s}T/Z_e\,z_x + T^2)}{1 + (k_d\,\mathrm{s} + k_p + k_i/\mathrm{s})K_V\,S_a\,(\mathrm{s}T/[Z_e\,z_x + T^2])}$$

which reduces to

$$\frac{a}{V_r}(\mathrm{s}) = \frac{\mathrm{s}(k_d\,\mathrm{s}^2 + k_p\,\mathrm{s} + k_i)K_V\,T}{(L_e\,m_x + k_d\,K_V\,S_a\,T)\mathrm{s}^3 + (L_e\,b_x + R_e\,m_x + k_p\,K_V\,S_a\,T)\mathrm{s}^2 + (L_e\,k_x + R_e\,b_x + T^2 + k_i\,K_V\,S_a\,T)\mathrm{s} + R_e\,k_x}. \tag{8}$$

The transfer function for output acceleration from a given input disturbance acceleration is given as

$$\frac{a}{a_d}(\mathrm{s}) = \frac{1}{1 + (k_d\,\mathrm{s} + k_p + k_i/\mathrm{s})K_V\,S_a\,(\mathrm{s}T/[Z_e\,z_x + T^2])}$$

which reduces to

$$\frac{a}{a_d}(\mathrm{s}) = \frac{L_e\,m_x\,\mathrm{s}^3 + (L_e\,b_x + R_e\,m_x)\mathrm{s}^2 + (L_e\,k_x + R_e\,b_x + T^2)\mathrm{s} + R_e\,k_x}{(L_e\,m_x + k_d\,K_V\,S_a\,T)\mathrm{s}^3 + (L_e\,b_x + R_e\,m_x + k_p\,K_V\,S_a\,T)\mathrm{s}^2 + (L_e\,k_x + R_e\,b_x + T^2 + k_i\,K_V\,S_a\,T)\mathrm{s} + R_e\,k_x}. \tag{9}$$

Note that equations (8) and (9) have the same characteristic equations (same denominators) and that the control parameters appear as coefficients of different powers of s (which contains the frequency). Thus, it can be expected that derivative feedback will be most helpful at reducing harmonics at the high frequencies. Similarly, k_p will be most useful at medium to high frequencies and k_i will help in the low to medium frequency range.

Classical stability analysis might be applied to these characteristic equations. However, it was not done in this study owing to the variability of coefficients with excitation frequency, excitation amplitude, magnetic bias point, material prestress, and even actuator load (T changes with different loads in the presence of eddy currents [2]). Reasonable estimates of stability criteria might be obtained by using empirical and/or analytical relationships for L_e, R_e, b_x, k_x, and T, as functions of all of the parameters mentioned previously, if they all existed. However, models of the functional trends in the behavior of system parameters with changes in operating conditions are not available. Nonetheless, as will be shown, parameter estimates for a fixed input drive magnitude and frequency can be measured and used to provide reasonable models of both the system open loop and closed loop system behaviour, *as run*. (Note that until such time as improved material models become available, an empirical approach to parameter estimation is advised. Measure parameters over the range of operating conditions of interest to determine whether or not the parameters change; use appropriate parameters for control under different operating conditions.) Awaiting further research into those relationships, the work presented demonstrates the improvements achievable without addressing stability issues, which were resolved empirically by restricting gains to values below those which produced instabilities.

Models have been developed for prediction of magnetostrictive transducer behaviour using a PID controller in the forward loop. It has been assumed that the transducer was a linear system which satisfied the pair of simultaneous equations (1), with the harmonic frequencies (that are known to exist) modelled as disturbance inputs. The primary goal of this endeavour is to reduce the harmonic signal content of the magnetostrictive transducer; thus extending its linear range to larger displacements, velocities, and

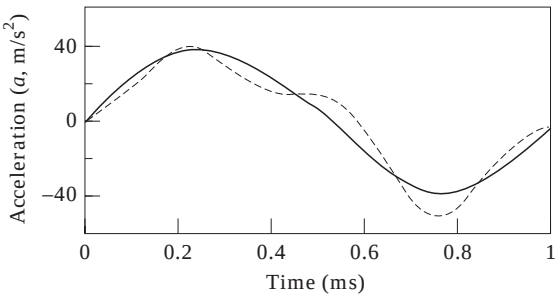

Figure 4. Experimental time traces of output acceleration; ——, proportional control; – – –, no control. Tests were run at 1000 Hz, 1/4 ampere (0–pk).

accelerations. To test the modelling technique, a PD controller was fabricated and experimental measurements were performed.

3. RESULTS

In this section, experimental evidence is offered to show that the control system generally improves the linearity of the transducer. Also, realities of the circuits and components employed will be discussed (including procedures for obtaining transducer parameters) and model predictions will be compared with experimental measurements of magnetostrictive transducer behaviour. Emphasis is placed on voltage-control.

3.1. TRENDS

An example of the effects of simple proportional feedback on the output acceleration of the transducer is shown in Figure 4. In the figure are two different experimental measurements of transducer output acceleration as functions of time. For both tests, the transducer was driven by a 1000 Hz, 1/4 amp drive current. As shown in the figure, the proportional feedback made a significant difference in the output wave form. Note that the second harmonic frequency component (3000 Hz) was reduced dramatically by simple proportional feedback.

Figure 5 shows experimental acceleration amplitudes for controlled (simple proportional acceleration feedback) and uncontrolled cases of three different drive current amplitudes. In all cases the drive current was oscillating at 1000 Hz. The other frequencies were

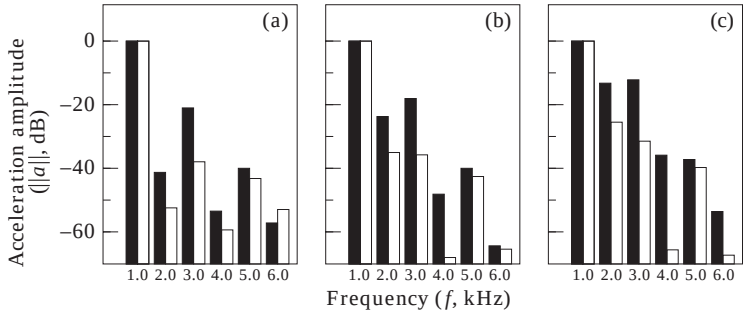

Figure 5. Experimental acceleration amplitudes resulting from 1000 Hz drive currents at three different amplitudes: (a) 23 mA, (b) 115 mA, (c) 250 mA. Data were taken from acceleration autospectral density functions. The percent harmonic distortion was calculated as $100 \times (\Sigma$ all amplitudes -1000 Hz amplitude$)/\Sigma$ all amplitudes. ■, No control; □, control.

TABLE 1

Percent harmonic distortion (%HD) of output acceleration; input frequency was 1000 Hz

	Drive current (I mA)		
	80	150	250
%HD with no feedback	13	19	32
%HD with low feedback gain	5	7	12
%HD with high feedback gain	3	5	9

harmonics. Each set of data was normalized by its acceleration amplitude at 1000 Hz (thus all show 0 dB at 1000 Hz). As shown in the figure, proportional acceleration feedback control generally decreased the harmonic amplitudes, over this frequency range, when compared with the corresponding uncontrolled drive current test. Note that at 4 kHz for the 250 mA drives, the controlled harmonic is approximately 30 dB below the uncontrolled case. Note also that for this range of drive currents the largest harmonic for the controlled cases is about 25 dB down; for the uncontrolled cases the largest is approximately -12 dB. The amplification of the 6000 Hz data in the 23 mA case may be a result of the combination of a low signal level at 55 dB below the 23 mA fundamental excitation level (i.e., the uncontrolled harmonic falling within the noise floor of the analogue components used) and a degradation in phase accuracy with increased frequency of both the analogue components and the amplifier used.

Data in Table 1 was calculated from experimental measurements like those shown in Figure 5 (the 250 mA high gain data is that shown in the figure). For these tests, two different proportional gains (the "low" gain was approximately half of the "high" gain) were used at three different amplitude, 1000 Hz drive currents. In all cases, increasing the proportional feedback reduces the harmonic distortion and the distortions increase with increasing drive current amplitudes. The second trend is in agreement with that shown in Figure 1 and implied by Figure 5. During the course of this study, the first trend was repeatedly observed experimentally (until the onset of instabilities). Note that the 250 mA high feedback case had lower distortion than that of the 80 mA uncontrolled case.

3.2. TRANSDUCER–CONTROLLER SYSTEM MODELLING

The input–output relationship for the Techron 7520 amplifier was measured. (The amplifier was fitted with a 75A08 control module, set for voltage control.) The system behaved somewhat like a first order system with a -3 dB point at about 57 kHz. Unless specified otherwise, it was modelled as a constant gain with a linear phase lag over the appropriate frequency range (usually 0 to 6 or 10 kHz).

The analogue control circuit was built in-house. Input–output relationships for each stage of the circuit were measured and compared with the theoretical relationships. Theory and experiment were found to be in excellent agreement. However, difficulties were encountered. The resonant frequency of the accelerometer as mounted was at 47 kHz. This frequency was fed back to the controller along with the disturbances that the system was designed to cancel. It seemed that the transducer output harmonics almost always contained a component sufficiently near 47 kHz to excite the accelerometer resonance. It was necessary to place a band-pass filter between the accelerometer and the summing amplifier in order to avoid feeding back and oscillating (it was also needed to block the

low frequency drift of the accelerometer signal conditioner). The transfer function for this filter was

$$\frac{V_{out}}{V_{in}}(\mathrm{s}) = \frac{\mathrm{s}R_2 C_2}{\mathrm{s}C_2\{R_1(\mathrm{s}R_2 C_1 + C_1/C_2 + 1) + R_2\} + 1}, \tag{10}$$

where $R_1 = 30\ \mathrm{k}\Omega$, $R_2 = 100\ \mathrm{k}\Omega$, $C_1 = 1000\ \mathrm{pF}$, and $C_2 = 0{\cdot}1\ \mu\mathrm{F}$. Its lower -3 dB frequency was 10 Hz; its upper was 7000 Hz. (This filter had a strong influence on the behaviour of the control system. As is shown later, it modified magnitudes and phases when compared with simulations from which it was omitted.) Since this filter was placed in the feedback loop, it can be thought of as modifying the sensitivity of the accelerometer. Therefore, everywhere S_a appears in equations (8) and (9), one should use the quantity $S_a \times$ equation (10).

The differentiator built for this investigation was simply an active first order band-pass filter with an adjustable gain. (See, for example, reference [10].) Its transfer function, assuming the op amps to be ideal, was

$$\frac{V_{out}}{V_{in}}(\mathrm{s}) = \frac{\mathrm{s}R_2 C_1}{(\mathrm{s}R_2 C_2 + 1)(\mathrm{s}R_1 C_1 + 1)} \times \text{adjustable gain}, \tag{11}$$

where $R_1 = 2{\cdot}2\ \mathrm{k}\Omega$, $R_2 = 10\ \mathrm{k}\Omega$, $C_1 = 0{\cdot}01\ \mu\mathrm{F}$, and $C_2 = 470\ \mathrm{pF}$. The phase on the output was $+90^\circ$ at low frequencies, reducing to $+45^\circ$ at 5075 Hz, i.e., its first -3 dB frequency was 5075 Hz. The proportional plus derivative summing amplifier also included an adjustable gain. Its effects on k_p and k_d were included in the reported values. Since the differentiator was not a pure derivative, $\mathrm{s}k_d$ values in equations (8) and (9) were replaced with

$$\mathrm{s}k_d/\{(\mathrm{s}R_2 C_2 + 1)(\mathrm{s}R_1 C_1 + 1)\}.$$

The reported values of k_d were calculated as the product of $R_2 C_1 \times$ adjustable gain $\times$ summing gain.

At this point, circuit parameters were known. The transducer was mass loaded such that the first axial mechanical resonance occurred between 2500 and 4000 Hz for all tests discussed. Unfortunately, the transducer used in this study had a radial mode of vibration which affected transducer axial behaviour around 7 kHz. As a result, model values reported (which are based on a 1-DOF mechanical model) are limited to frequencies less than 6 kHz.

Quantities applicable to the magnetostrictive transducer must be estimated in order to model the transducer behaviour. One needs estimates of T, the transduction coefficient, Z_e, the blocked electrical impedance of the transducer, and z_x, the sum of the mechanical impedances of the transducer and the load. One might consult the literature for "nominal" material properties, or build a transducer and measure them. Typical results from both methods are shown in Figure 6 for the case of simple proportional feedback control. Also, measured accelerometer voltage per unit input reference voltage were taken at several different input frequencies, and are indicated on the plots with an X. The figure shows the magnitude and phase of the product of S_a and equation (6) $= V_{acc}/V_r =$ accelerometer voltage over input or reference voltage.

In Figure 6, model 1 was calculated using published "nominal" Terfenol-D parameters [11], relations from the literature [6], and the details of the control circuit discussed above. The transduction coefficient was calculated as $T = NdE_y^H \pi r^2/l_r$, where $N =$ turns of the wound wire solenoid ($N = 1300$); $d =$ the linear coupling coefficient of the Terfenol-D rod ($d \approx 1{\cdot}5 \times 10^{-8}$ m/A); $E_y^H =$ Terfenol-D's Young's modulus measured at constant applied magnetic field ($E_y^H \approx 3{\cdot}0 \times 10^{10}$ Pa); $r =$ the radius of the Terfenol-D rod ($r = 3{\cdot}175$ mm); and $l_r =$ the rod length ($l_r = 0{\cdot}0508$ m). Thus, $T \approx 365$ N/A. The blocked electrical

impedance of the transducer, Z_e, was estimated as the DC resistance ($R_e \approx 6\ \Omega$) plus $j\omega L_e$, where $j = \sqrt{(-1)}$, $\omega = 2\pi f$ = frequency of oscillation in rad/s, and $L_e \approx \mu^\varepsilon n^2 \pi r_s^2 l_s = 2{\cdot}5\mu_0$ 23264^2 π $0{\cdot}00385^2$ $0{\cdot}0559 = 4{\cdot}43$ mH (μ^ε is the blocked magnetic permeability of Terfenol-D $\approx 2{\cdot}5\mu_0$, $\mu_0 = 4\pi \times 10^{-7}$ Tm/amp-turn, n is the number of turns per unit length of the solenoid, r_s is the inner radius of the solenoid, and l_s is the length of the solenoid). The mechanical impedance of the transducer, as loaded, was calculated using simple second order mechanical relations [12], i.e., $k_x = EA/l_r = E_y^H \pi r^2/l_r = 18{\cdot}7$ MN/m; m_x was measured = mass of the load plus some attaching components plus 1/3 the mass of the Terfenol-D rod ($m_x = 0{\cdot}086$ kg), $\omega_n = (k_x/m_x)^{1/2}$, and b_x was estimated based on a four percent damping coefficient, i.e., $b_x \approx 2 \times 0{\cdot}04\omega_n m_x$.

Model 1 ignores the presence and effects of eddy currents within the magnetostrictive rod, and uses simple formulas from physics and published values for material parameters. Considering these gross simplifications, the model 1 simulation shown in Figure 6 was thought to be surprisingly good, particularly when measured against open-loop models shown in reference [2]. Model 2, however, did a better job of matching the experimental measurements.

Model 2 in Figure 6 was calculated using the electrical impedance modelling technique developed in reference [2]. A brief outline of the technique follows. Transducer and material parameters are measured/inferred by electrical impedance and admittance analysis performed on experimental measurements of the transducer's electrical impedance and displacement from electric current functions. These functions are measured using a current control driver since material parameters are very sensitive to magnetic field strength drive levels. Thus, V/I and a variation on v/V are measured. From these measurements and knowledge of the mechanical aspects of the transducer under test (i.e., m_x, solenoid specifications, the stiffness of the prestress mechanism, electrical conductivities, and dimensions), one can calculate E_y^H, magnetomechanical coupling (k^2), the "d" constant, the mechanical damping coefficient (ζ), and the magnetic permeability at constant stress and/or constant strain. All of these parameters are used to calculate analytical solutions (a plethora of modified Bessel functions) for Maxwell's equations using a complex valued, frequency and load dependent "dynamic magnetic permeability" for the magnetostrictive material within the transducer. In this way, the effects of eddy currents in the magnetostrictive rod (and housing, if applicable) are included. An analytical solution for the electrical impedance of equation (3) is then calculated, i.e., one performs a simulation to calculate V/I including motional and eddy current effects. This calculated

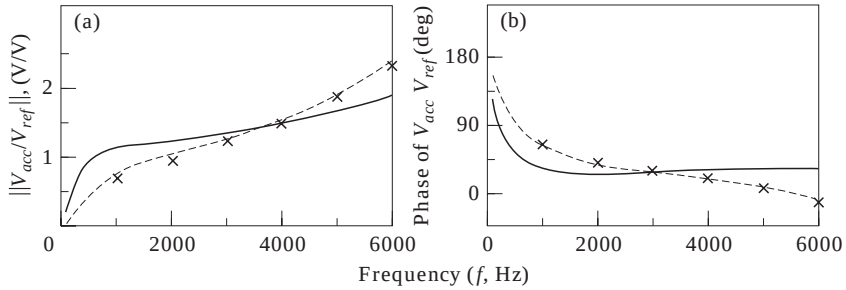

Figure 6. Predicted accelerometer voltage per unit reference voltage for proportional feedback control: (a) magnitude and (b) phase. Models are based on equation (6). Model 1 (——) used "nominal" material properties. Model 2 (– – –) used measured properties. 'X's indicate measured values of accelerometer voltage per unit reference voltage from sinusoidal input at different frequencies.

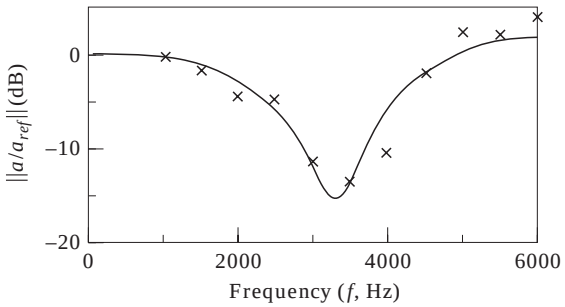

Figure 7. Output acceleration due to input disturbance accelerations using proportional feedback control, $k_p = 2{\cdot}73$ V/V; ——, model; ×, experiment.

V/I should be a reasonable approximation ($\pm 10\%$ in both magnitude and phase) of the experimental measurement performed earlier.

What remains to be done is to calculate the yet unknown coefficients, Z_e and T, which are needed for the controls modelling. One can calculate Z_e, the blocked electrical impedance of the transducer, *including* the effects of eddy currents, by calculating V/I again. However, this time through, use the measured/calculated value of the blocked magnetic permeability of the magnetostrictive material instead of the "dynamic magnetic permeability" which was used the first time through. The transduction coefficient, T, can now be calculated—including the effects of the load and frequency dependent eddy currents—by solving equation (3) for T, i.e., $[(V/I - Z_e)z_x]^{1/2} = T$.

The procedure outlined above was carried through one time with the transducer operated at a representative drive current amplitude and with a representative load. The process would likely need to be repeated if either the magnetic bias point or the prestress of the transducer was changed. However, they remained constant for the experiments which are compared with the model calculations.

It should be mentioned that a third method of estimating Z_e and T was tried, and it resulted in fairly reasonable approximations of the feedback control system behavior. One can measure V/I for the transducer, as run, perform a *linear* curve fit to the real and imaginary parts separately, and use the resulting empirical relations for $Z_e(f)$. These relations will include an approximation of the eddy current effects, i.e., the real part will be a function of frequency. One can then estimate T by solving equation (3) as above, only this time using the experimental measurement of V/I.

3.3. FEEDBACK CONTROL SYSTEM PERFORMANCE

Attention will now be paid to the effects of the feedback control system on the amplitudes of the harmonic accelerations. (Recall equation (9) for a/a_d.) For the experimental "measurements" of this function, one test was run at a given current amplitude at a single frequency (e.g., 0·15 A at 1000 Hz) without feedback control, followed by an otherwise identical test with feedback control. In each case, acceleration autospectral density functions were calculated over an extended frequency range (e.g., 0–10 000 Hz) in order to measure the harmonics. The experimental "measurement" of a/a_d was calculated as the difference, in dB, between the uncontrolled and the controlled experimental measurements.

Figure 7 displays experimental measurements (X) and model predictions (line) for simple proportional feedback control of the transducer. The model used was that of equation (9) for the reduction in disturbance (harmonic) acceleration amplitudes. Transducer parameters used in the simulation were obtained by the method of reference [2]. For both

experimental measurements (controlled and uncontrolled), the transducer was driven with a 0·25 amp, 500 Hz sinusoidal current. Thus, the first disturbance/harmonic would be at 1000 Hz, the second at 1500 Hz, the third at 2000 Hz, etc. The largest discrepancies between model and experiment occurred at 4000, 5000, and 6000 Hz. The experimental measurements at these frequencies were in excess of 60 dB below the fundamental's amplitude; thus, while still above the noise floor, they are suspect due to the instrumentation's dynamic range. For this test the mechanical resonant frequency was approximately 3200 Hz. Note the 15 dB attenuation near resonance and the increase in amplitude of the disturbance accelerations for 5000 Hz and above, and for frequencies below 1000 Hz.

The effects of including a derivative controller are seen by comparing Figures 7 and 8. Note that the differentiator improved the high frequency disturbance attenuation of the system. This trend was anticipated in the discussion below equation (9). As in Figure 7, the 4, 5, and 6 kHz experimental measurements in Figure 8 were more than 60 dB down, thus they are suspect. Note, however, the substantial agreement between experiment and the model simulation. It is also apparent from the data that adding differential feedback slightly increases the harmonic distortion at the lower frequencies and decreases the distortion as frequencies increase.

4. DISCUSSION

Now that some confidence exists that the models developed in this study yield predictions which resemble transducer behavior, the models are used to predict some performance trends. First, the influence of the band pass filter is removed. Recall that this filter was added to avoid feedback of a signal due to resonance of the accelerometer. Ideally this filter should have not affected the acceleration disturbances produced as a result of transducer non-linearities. Removing the filter simulates control using a low drift, low noise accelerometer and conditioner. This is done in the model by simply removing equation (10). Figure 9 shows magnitude and phase of acceleration per unit reference voltage for the PD controller conditions of Figure 8, with the band pass filter, as a solid line, and without the band pass filter, as a dotted line. Removal of the filter results in a fairly large improvement in output linearity, with a substantial shift towards constant magnitude apparent in the dashed line. It has the net effect of restoring the high frequency feedback signal. From almost 2000 Hz up to 6000 Hz a relatively constant acceleration per input reference voltage is exhibited and a phase angle closer to a zero is achieved.

In addition, Figure 9 illustrates the influence of an integrator, although no integrator was experimentally implemented. The dashed curves labeled "with integrator" show the

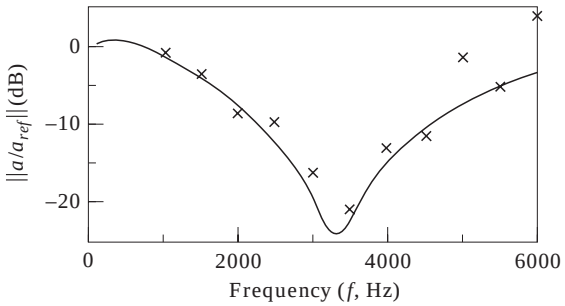

Figure 8. PD feedback control of magnetostrictive transducer, $k_p = 6{\cdot}2$ V/V, $k_d \approx 90 \times 10^{-6}$ Vs/V; ——, model; ×, experiment.

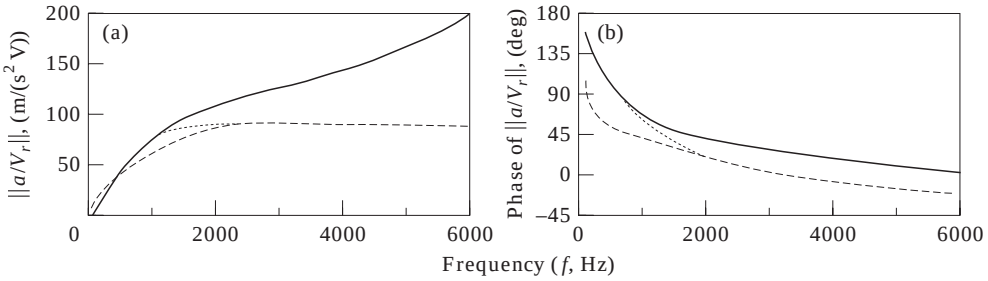

Figure 9. Predicted (a) magnitude and (b) phase for models of a/V_r for a cleaner accelerometer/conditioner and adding an integrator to the control algorithm. Starting point refers to the PD controller setting used in Figure 8. ——, Starting point; · · · ·, no filter; – – –, with integrator.

effects of adding a modest amount of integration to the "no filter" control algorithm. (Integrators are usually high gain, first order low pass active filters. The integrator modelled here had the transfer function: $1/(s \times 2{\cdot}2\ \text{k}\Omega \times 0{\cdot}1\ \mu\text{F} + 2{\cdot}2\ \text{k}\Omega/22\ \text{k}\Omega)$ $\times$ summing gain. The -3 dB point for this circuit was approximately 90 Hz, i.e., it resembled an integrator (1/s) for frequencies greater than 90 Hz. As presented, $k_i \approx 16\,500$ V/(sV).)

As shown in the figures, removing the filter would significantly improve output accelerations per unit reference voltage. Incorporating an integrator into the controller would improve the system behavior at the lower frequencies.

An alternative look at this trend is shown in Figure 10. The reduction of the magnitude of output acceleration due to input disturbance accelerations, with filter removal helping reduce a/a_d above roughly 1500 Hz, and the integrator helping between 900 and roughly 2000 Hz. The addition of the integrator and removal of the filter ensure that harmonic frequencies will be reduced over the whole frequency range of the study (it removed the characteristic hump below 1 kHz of the previous implementations).

The addition of an acceleration feedback control system improves the linearity (reduces harmonic distortion) of the output of a magnetostrictive transducer. In one case, 32% harmonic distortion was decreased to 9% via simple proportional feedback control. This improvement translates to increasing the magnitude of the low distortion, linear range displacements by a factor of approximately 15 (when compared to the uncontrolled transducer). Thus, simple feedback control has been demonstrated to increase the "linear range" of transducer outputs. Harmonics occurring at frequencies near the mechanical

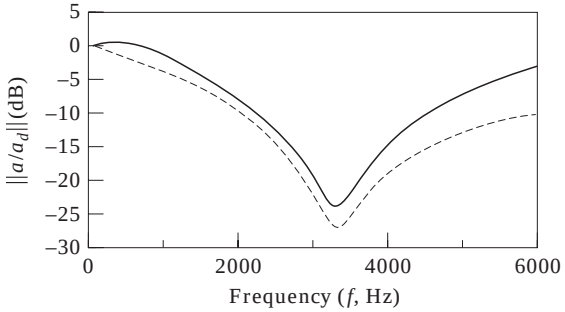

Figure 10. Model predictions of the output acceleration magnitude due to input disturbance accelerations. Starting point refers to the PD controller setting used in Figure 8, with a band pass filter and no integrator. ——, Starting point; · · · ·, no filter; – – –, with integrator.

resonant frequency of the loaded transducer show the greatest attenuations (approaching 30 dB in this study). Differential feedback tended to increase harmonics at the lower frequencies and decrease those occurring at the higher frequencies. Modelling implies that adding an integrator to the control algorithm would tend to reduce the low frequency harmonics.

5. CONCLUSIONS

The utility of simple analog feedback control for the linearization of non-linear magnetostrictive transducers has been demonstrated experimentally. Both proportional and proportional plus derivative acceleration feedback control were shown to reduce the harmonic frequency content of the transducer; though not in a simple or intuitive way. Thus, attentions were turned to developing models to predict and explain the behavior of the closed loop system.

Using only simple linear systems relations (linear feedback control and transduction theories), expressions were developed for predicting closed loop system behavior. Specifically, two cases were examined. In the first it was assumed that a current control amplifier of appreciable robustness were used. There, expressions were developed for output displacement from input reference voltage, $u/V_r(s)$, and output displacement from input disturbance displacement, $u/u_d(s)$. Equipment problems forbade experimental verification of those expressions. For the second case, that of a voltage control amplifier, expressions were developed for output acceleration from input reference voltage, $a/V_r(s)$, and output acceleration from input disturbance acceleration, $a/a_d(s)$. These expressions were experimentally verified. Thus, one can, with confidence, analytically model the behaviour of the closed loop system predicting the observed reductions in output harmonics and predicting the "desired" system output as a function of frequency.

Three methods one might use to estimate magnetostrictive transducer model parameters were presented. Model predictions from two of the methods were compared with experimental measurements. The more elaborate method, that which included the effects of eddy currents within the transducer, produced the better of the two closed loop model predictions.

The analytical expressions previously developed were used to explore system behaviour under the assumptions that one used better components and then added an integrator to the controller. Model predictions indicate that there is a lot to be gained by employing both an integrator and higher quality components. The techniques developed in this paper are applicable to general vibration control applications that employ magnetostrictive transducers.

ACKNOWLEDGMENTS

We would like to acknowledge financial support of this study by the National Science Foundation. Support was provided through a Research Initiation Award, MSS-9212065, and a Young Investigator Award, CMS-9457288. Our thanks to Tad Calkins and Rick Zrostlik, for their input and patience, to Chad Bouton who gave up space, capacitors, and serenity in service to this research, and to Toby Hansen and Kevin Shoop at Edge Technologies, Inc., for their magnetization, availability, and parts services.

REFERENCES

1. F. V. Hunt 1982 *Electroacoustics*: *the Analysis of Transduction*, *and its Historical Background*. Woodbury, NY: Acoustical Society of America.
2. D. L. Hall 1994 *PhD Dissertation*, *Iowa State University*, *Ames*, *IA*. Dynamics and vibrations of magnetostrictive transducers.
3. A. E. Clark 1980 *Ferromagnetic Materials* (Editor, E. P. Wohlfarth) Amsterdam: North-Holland Publishing **1**, chapter 7, 531–589. Magnetostrictive rare earth-Fe_2 compounds.
4. A. E. Clark, J. P. Teter, M. Wun-Fogle, M. B. Moffett and J. Lindberg 1990 *Journal of Applied Physics* **67**, 5007–5009. Magnetomechanical coupling in Bridgman-Grown $Tb_{0.3}\,Dy_{0.7}\,Fe_{1.9}$ at high drive levels.
5. *International Electrotechnical Commission IEC Report*, *Publication* 782, 1984. Measurements of ultrasonic magnetostrictive transducers.
6. D. L. Hall and A. B. Flatau 1995 *Journal of Intelligent Materials Systems and Structures* **6**, 315–328. One-dimensional analytical constant parameter linear electromagnetic–magnetomechanical models of a cylindrical magnetostrictive (Terfenol-D) transducer.
7. G. F. Franklin, J. D. Powel and A. Emami-Naeini 1986 *Feedback Control of Dynamic Systems*. Reading, MA: Addison-Wesley, 113–118.
8. M. J. Dapino, F. T. Calkins, D. L. Hall and A. B. Flatau 1996 *SPIE Proceedings on Smart and Integrated Systems* **2717**, Paper 66, 697–708. Measured Terfenol-D material properties under varied operating conditions.
9. F. T. Calkins, M. J. Dapino and A. B. Flatau 1997 *Proceedings on Smart Structures and Integrated Systems* **304,** 293–304. Effect of Prestress on Terfenol-D Material Properties.
10. P. Horowitz and W. Hill 1989 *The Art of Electronics*. Cambridge: Cambridge University Press; second edition, 224, 5.
11. Edge Technologies, Inc. 1988 *Typical Material Properties*, Ames, IA: Edge Technologies.
12. M. L. James, G. M. Smith, J. C. Wolford and P. W. Whaley 1989 *Vibration of Mechanical and Structural Systems*: *with Microcomputer Applications*. New York: Harper and Row.